arXiv:1606.01769v1 [gr-qc] 6 Jun 2016

Inspiral waveforms for spinning compact binaries in a new precessing convention

Anuradha Gupta[1] **and Achamveedu Gopakumar**[2]

[1]Inter University Centre for Astronomy and Astrophysics, Ganeshkhind, Pune 411007, India
[2]Department of Astronomy and Astrophysics, Tata Institute of Fundamental Research, Mumbai 400005, India

E-mail: anuradha@iucaa.in

Abstract. It is customary to use a precessing convention, based on Newtonian orbital angular momentum $\boldsymbol{L}_{\rm N}$, to model inspiral gravitational waves from generic spinning compact binaries. A key feature of such a precessing convention is its ability to remove all spin precession induced modulations from the orbital phase evolution. However, this convention usually employs a post-Newtonian (PN) accurate precessional equation, appropriate for the PN accurate orbital angular momentum $\boldsymbol{L}$, to evolve the $\boldsymbol{L}_{\rm N}$-based precessing source frame. This motivated us to develop inspiral waveforms for spinning compact binaries in a precessing convention that explicitly use $\boldsymbol{L}$ to describe the binary orbits. Our approach introduces certain additional 3PN order terms in the orbital phase and frequency evolution equations with respect to the usual $\boldsymbol{L}_{\rm N}$-based implementation of the precessing convention. The implications of these additional terms are explored by computing the match between inspiral waveforms that employ $\boldsymbol{L}$ and $\boldsymbol{L}_{\rm N}$-based precessing conventions. We found that the match estimates are smaller than the optimal value, namely 0.97, for a non-negligible fraction of unequal mass spinning compact binaries.

1. Introduction

Inspiralling compact binaries containing spinning black holes (BHs) are plausible sources for the network of second generation gravitational wave (GW) detectors like the advanced LIGO (aLIGO), advanced Virgo, KAGRA, GEO-HF and the planned LIGO-India [1]. The inspiral dynamics and associated GWs from compact binaries can be accurately described using the post-Newtonian (PN) approximation to general relativity [2]. Moreover, an optimal detection technique of *matched filtering* is employed to detect and characterize inspiral GWs from such binaries. In this technique, one cross correlates the interferometric output data with a bank of templates that theoretically model inspiral GWs from spinning binaries. The construction of these templates involves modeling the two GW polarization states, $h_{\times}(t)$ and $h_{+}(t)$, associated with such events, in an accurate and efficient manner. At present, GW frequency and associated phase evolution, crucial inputs to compute $h_{\times,+}(t)$, are known to 3.5PN order for non-spinning compact binaries [3] whereas the amplitudes are available to 3PN order [4]. In the case of spinning components, the spin effects enter the dynamics and GW emission via spin-orbit (SO) and spin-spin (SS) interactions [5]. Additionally, $\boldsymbol{S}_1$, $\boldsymbol{S}_2$ and $\boldsymbol{L}$, the two spin and orbital angular momenta, for generic spinning compact binaries precess around the total angular momentum $\boldsymbol{J} = \boldsymbol{L} + \boldsymbol{S}_1 + \boldsymbol{S}_2$ due to SO and SS interactions. This forces substantial modulations of the emitted GWs from inspiralling generic spinning compact binaries [6, 7]. Therefore, it is

important to incorporate various spin effects while constructing inspiral GW templates for spinning compact binaries. At present, GW frequency evolution and amplitudes of $h_{\times,+}(t)$ for maximally spinning BH binaries are fully determined to 2.5PN and 2PN orders, respectively, while incorporating all the relevant spin induced effects [6, 8].

There exist inspiral waveforms for precessing binaries, implemented in the LALSIMULATION package of LIGO Scientific Collaboration (LSC) [9], that employ the *precessing convention* of [10]. An attractive feature of this convention is its ability to remove all the spin precession induced modulations from the orbital phase evolution. This allows one to express the orbital phase $\Phi_p(t)$ as an integral of the orbital frequency $\omega(t)$, namely $\Phi_p(t) = \int \omega(t)\, dt$. Therefore, in this convention, the inspiral waveform from precessing binaries can be written as the product of a non-precessing carrier waveform and a modulation term that contains all the precessional effects. The convention involves a *precessing source frame* $(\boldsymbol{e}^l_1, \boldsymbol{e}^l_2, \boldsymbol{e}^l_3 \equiv \hat{\boldsymbol{L}}_{\rm N})$ whose basis vectors satisfy the evolution equations $\dot{\boldsymbol{e}}^l_{1,2,3} = \boldsymbol{\Omega}^l_e \times \boldsymbol{e}^l_{1,2,3}$. The angular frequency Ω^l_e is constructed in such a manner that the three basis vectors $\boldsymbol{e}^l_1, \boldsymbol{e}^l_2$ and $\hat{\boldsymbol{L}}_{\rm N}$ always form an orthonormal triad. Subsequently, $\boldsymbol{\Omega}^l_e$ has to be $\boldsymbol{\Omega}^l_e = \boldsymbol{\Omega}_k - (\boldsymbol{\Omega}_k \cdot \hat{\boldsymbol{L}}_{\rm N})\hat{\boldsymbol{L}}_{\rm N}$, where Ω_k is the usually employed precessional frequency for $\boldsymbol{L}_{\rm N}$. The relevant expression for $\boldsymbol{\Omega}_k$ can be obtained by collecting the terms that multiply $\hat{\boldsymbol{L}}_{\rm N}$ in equation (9) in [10]. This triad defines an orbital phase $\Phi_p(t)$ such that $\boldsymbol{n} = \cos\Phi_p\, \boldsymbol{e}^l_1 + \sin\Phi_p\, \boldsymbol{e}^l_2$, where $\boldsymbol{n}$ is the unit vector along binary separation vector $\boldsymbol{r}$. Furthermore, one can express $\dot{\boldsymbol{n}}$ in the co-moving frame $(\boldsymbol{n}, \boldsymbol{\lambda} = \hat{\boldsymbol{L}}_{\rm N} \times \boldsymbol{n}, \hat{\boldsymbol{L}}_{\rm N})$ as $\dot{\boldsymbol{n}} = \dot{\Phi}_p \boldsymbol{\lambda} + \boldsymbol{\Omega}^l_e \times \boldsymbol{n}$. It was argued in [10] that $\boldsymbol{\Omega}^l_e$ should only be proportional to $\boldsymbol{n}$, leading to $\dot{\boldsymbol{n}} = \dot{\Phi}_p \boldsymbol{\lambda}$. Thus, the adiabatic condition for the sequence of circular orbits, namely $\dot{\boldsymbol{n}} \cdot \boldsymbol{\lambda} = \omega$, gives the desired result, i.e., $\dot{\Phi}_p = \omega$. It should be obvious that the above adiabatic condition can also imply $\dot{\boldsymbol{n}} \cdot \dot{\boldsymbol{n}} = \omega^2$.

In practice, the precessional equation for $\boldsymbol{L}$ is employed to construct $\boldsymbol{\Omega}^l_e$ and to evolve $\boldsymbol{L}_{\rm N}$. As a consequence, $\boldsymbol{\Omega}^l_e$ is no longer proportional to $\boldsymbol{n}$ [11] and this leads to PN corrections to $\dot{\Phi}_p = \omega$ (see section 2.1 of [12] for detailed calculation). These observations motivated us to provide a set of PN accurate equations to obtain temporally evolving quadrupolar order $h_{\times,+}$ for generic spinning compact binaries in an $\boldsymbol{L}$-based precessing convention. In the next section, we present our $\boldsymbol{L}$-based precessing convention and explore its data analysis implications in the later section.

2. Inspiral waveforms via an $\boldsymbol{L}$-based precessing convention

In this section, we introduce a $\boldsymbol{k}$-based precessing source frame ($\boldsymbol{e}_1$,$\boldsymbol{e}_2$, $\boldsymbol{e}_3 \equiv \boldsymbol{k}$), to develop a $\boldsymbol{k}$-based precessing convention, where $\boldsymbol{k}$ is unit vector along $\boldsymbol{L}$. The precessional dynamics of $\boldsymbol{e}_1, \boldsymbol{e}_2$ and $\boldsymbol{e}_3$ are provided by $\dot{\boldsymbol{e}}_{1,2,3} = \boldsymbol{\Omega}_e \times \boldsymbol{e}_{1,2,3}$, where $\boldsymbol{\Omega}_e \equiv \boldsymbol{\Omega}_k - (\boldsymbol{\Omega}_k \cdot \boldsymbol{k})\, \boldsymbol{k}$ and Ω_k is the usual precessional frequency of $\boldsymbol{k}$. It should be obvious that $\dot{\boldsymbol{e}}_3 = \boldsymbol{\Omega}_e \times \boldsymbol{e}_3$ is identical to $\dot{\boldsymbol{e}}_3 = \boldsymbol{\Omega}_k \times \boldsymbol{e}_3$ as $\boldsymbol{e}_3 \equiv \boldsymbol{k}$. It is possible to construct a $\boldsymbol{k}$-based co-moving triad $(\boldsymbol{n}, \boldsymbol{\xi} = \boldsymbol{k} \times \boldsymbol{n}, \boldsymbol{k})$ and define an orbital phase Φ such that $\boldsymbol{n} = \cos\Phi\, \boldsymbol{e}_1 + \sin\Phi\, \boldsymbol{e}_2$ and $\boldsymbol{\xi} = -\sin\Phi\, \boldsymbol{e}_1 + \cos\Phi\, \boldsymbol{e}_2$. Also, the time derivatives of $\boldsymbol{n}$ is given by $\dot{\boldsymbol{n}} = \dot{\Phi}\, \boldsymbol{\xi} + \boldsymbol{\Omega}_e \times \boldsymbol{n}$. Consequently, the frame independent adiabatic condition for circular orbits, namely $\dot{\boldsymbol{n}} \cdot \dot{\boldsymbol{n}} \equiv \omega^2$, leads to $\omega^2 = \dot{\Phi}^2 + \Omega^2_{e\xi}$, where $\Omega_{e\xi} = \boldsymbol{\Omega}_e \cdot \boldsymbol{\xi}$. This results in the following 3PN accurate differential equation for Φ,

$$\dot{\Phi} = \frac{c^3}{G\,m}\, x^{3/2} \left\{ 1 - \frac{x^3}{2} \left[\delta_1\, q\, \chi_1\, (\boldsymbol{s}_1 \cdot \boldsymbol{\xi}) + \frac{\delta_2}{q}\, \chi_2\, (\boldsymbol{s}_2 \cdot \boldsymbol{\xi}) \right]^2 \right\}, \tag{1}$$

where $q = m_1/m_2$, $\delta_{1,2} = \eta/2 + 3\,(1 \mp \sqrt{1-4\eta})/4$, $\eta = m_1\, m_2/m^2$ and $m = m_1 + m_2$. The PN expansion parameter x is defined as $(G\, m\, \omega/c^3)^{2/3}$. The Kerr parameters χ_1 and χ_2 of the two compact objects of mass m_1 and m_2 specify their spin angular momenta by $\boldsymbol{S}_{1,2} = G\, m^2_{1,2}\, \chi_{1,2}\, \boldsymbol{s}_{1,2}/c$, where $\boldsymbol{s}_1$ and $\boldsymbol{s}_2$ are the unit vectors along $\boldsymbol{S}_1$ and $\boldsymbol{S}_2$. The use of $\boldsymbol{L}$ to describe binary orbits also modifies the evolution equation for ω (or x). This is because the SO interactions are usually incorporated in terms of $\boldsymbol{s}_1 \cdot \boldsymbol{l}$ and $\boldsymbol{s}_2 \cdot \boldsymbol{l}$, in the literature [6, 10].

These terms require modifications due to the 1.5PN order relation between $\boldsymbol{l}$ and $\boldsymbol{k}$ which can be obtained from equation (8) in [12]. The PN accurate expression for $\dot{x}$ along with the 3PN additional terms is given by equation (9) in [12]. Notice that these additional terms are, for example, with respect to equation (3.16) in [13] that provides PN accurate expression for $\dot{x}$ while invoking $\boldsymbol{l}$ to describe binary orbits.

We now model inspiral GWs from spinning binaries in our $\boldsymbol{k}$-based precessing convention. The expressions for quadrupolar order $h_\times$ and h_+, written in the frame-less convention [6], read

$$h_\times|_{\rm Q}(t) = 2\,\frac{G\,m\,\eta\,x}{c^2\,R'}\,(2\,\xi_x\,\xi_y - 2\,n_x\,n_y)\,, \tag{2a}$$

$$h_+|_{\rm Q}(t) = 2\,\frac{G\,m\,\eta\,x}{c^2\,R'}\,(\xi_x^2 - \xi_y^2 - n_x^2 + n_y^2)\,, \tag{2b}$$

where $\xi_{x,y}$ and $n_{x,y}$ are the x and y components of $\boldsymbol{\xi}$ and $\boldsymbol{n}$ in an inertial frame associated with $\boldsymbol{N}$, the unit vector that points from the source to the detector, while R' is the distance to the binary. These x and y components of $\boldsymbol{\xi}$ and $\boldsymbol{n}$ can be expressed in terms of the Cartesian components of $\boldsymbol{e}_1$ and $\boldsymbol{e}_2$. In order to obtain $h_\times|_{\rm Q}(t)$ and $h_+|_{\rm Q}(t)$, we require to solve numerically the differential equations for $\Phi, x, \boldsymbol{e}_1$ and $\boldsymbol{e}_2$. We use equation (1) for Φ while the differential equation for x, $\boldsymbol{e}_1$ and $\boldsymbol{e}_2$ are given by equations (9) and (13) in [12]. It easy to see that the evolution of $\boldsymbol{e}_1$ and $\boldsymbol{e}_2$ depends upon the time variation of $\boldsymbol{s}_1$, $\boldsymbol{s}_2$ and $\boldsymbol{k}$. Therefore, we also need to solve differential equations for $\boldsymbol{s}_1$, $\boldsymbol{s}_2$ and $\boldsymbol{k}$. These differential equations that include the leading order SO and SS interactions can be obtained from equation (15) in [12].

In practice, we numerically solve the differential equations for $\boldsymbol{e}_1, \boldsymbol{k}$, $\boldsymbol{s}_1$, $\boldsymbol{s}_2$, Φ and x to obtain temporally evolving Cartesian components of $\boldsymbol{\xi}$ and $\boldsymbol{n}$. Note that we do not solve the differential equation for $\boldsymbol{e}_2$. This is because the temporal evolution of $\boldsymbol{e}_2$ can be estimated using the relation $\boldsymbol{e}_2(t) = \boldsymbol{k}(t) \times \boldsymbol{e}_1(t)$. The required initial values for the Cartesian components of $\boldsymbol{e}_1$, $\boldsymbol{k}$, $\boldsymbol{s}_1$ and $\boldsymbol{s}_2$ are given by freely choosing the following five angles: θ_{10}, ϕ_{10}, θ_{20}, ϕ_{20} and ι_0. The initial Cartesian components of $\boldsymbol{s}_1$, $\boldsymbol{s}_2$, $\boldsymbol{k}$ and $\boldsymbol{e}_1$ as functions of the above angles are given by equations (16) in [12]. Note that this choice of initial conditions is influenced by the LALSUITE SpinTaylorT4 code of LSC. Additionally, we let the initial x value to be $x_0 = (G\,m\,\omega_0/c^3)^{2/3}$ where $\omega_0 = 10\pi$ Hz (relevant for aLIGO) and the initial phase Φ_0 to be zero. In what follows, we explore the data analysis implications of these inspiral waveforms that employ the $\boldsymbol{L}$-based precessing convention.

3. Implications of inspiral waveforms in $\boldsymbol{L}$-based precessing convention

We employ the *match* [14] to compare inspiral waveforms constructed via the $\boldsymbol{l}$ and $\boldsymbol{k}$-based precessing conventions. Our comparison is influenced (and justified) by the fact that the precessing source frames of these two conventions are functionally identical. This should be evident from the use of *the same* precessional frequency, appropriate for $\boldsymbol{k}$, to obtain PN accurate expressions for both the $\boldsymbol{l}$-based $\boldsymbol{\Omega}_e^l$ and $\boldsymbol{k}$-based $\boldsymbol{\Omega}_e^l$. Therefore, the *match* estimates probe influences of the additional 3PN order terms present in the differential equations for Φ and x in our approach. Note that these 3PN order terms are not present in the usual implementation of the precessing convention as provided by the LALSUITE SpinTaylorT4 code.

Our match $\mathcal{M}(h_l, h_k)$ computations involve h_l and h_k, the two families of inspiral waveforms arising from the $\boldsymbol{l}$ and $\boldsymbol{k}$-based precessing conventions. The h_l inspiral waveform families are adapted from the LALSUITE SpinTaylorT4 code of LSC while h_k families arise from our approach (equations (2)). We employ the quadrupolar order expressions for $h_{\times,+}$ while computing h_l and h_k in the present analysis. Moreover, the two families are characterized by identical values of m, η, χ_1 and χ_2. Also, the initial orientations of the two spins in the $\boldsymbol{N}$-based inertial frame are also chosen to be identical. The computation of $\boldsymbol{N}\cdot\boldsymbol{l}$ from $\boldsymbol{N}\cdot\boldsymbol{k}$ with the help of equation (8) in

[12] ensures that $\boldsymbol{l}$ and $\boldsymbol{k}$ orientations at the initial epoch are physically equivalent. Therefore, our match computations indeed compare two waveform families with physically equivalent orbital and spin configurations at the initial epoch. Note that we terminate h_l and h_k inspiral waveform families when their respective x parameters reach 0.1 ($r \sim 10\,G\,m/c^2$).

Figure 1 represents the result of our $\mathcal{M}$ computations. The binary configurations have initial dominant SO misalignments $\tilde{\theta}_1(x_0)$ ($\cos^{-1}(\boldsymbol{k}\cdot\boldsymbol{s}_1)$) as 30° and we let the initial orbital plane orientation in the $\boldsymbol{N}$-based inertial frame to take two values leading to edge-on ($\iota_0 = 90°$) and face-on ($\iota_0 = 0°$) binary orientations. For these two configurations, we need to choose θ_{10} to be 30° and 60°, respectively. Moreover, we choose $\phi_{10} = 0°$, $\theta_{20} = 20°$, $\phi_{20} = 90°$. Let us note that $\boldsymbol{l}$ orientations (from $\boldsymbol{N}$) for these configurations will be slightly different from 0° or 90° due to the 1.5PN accurate relation between $\boldsymbol{l}$ and $\boldsymbol{k}$.

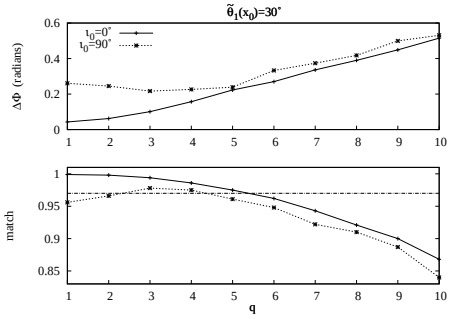

Figure 1. Plots for the accumulated orbital phase ($\Delta\Phi$) and the associated match ($\mathcal{M}$) estimates as functions of the mass ratio q for maximally spinning $m = 30M_\odot$ BH binaries inspiralling in the $[x_0, 0.1]$ frequency interval.

We also plot $\Delta\Phi$, the accumulated orbital phase differences in the frequency interval $[x_0, 0.1]$. We find that the variations in $\mathcal{M}$ estimates are quite independent of the initial orbital plane orientations. We see a gradual decrease in $\mathcal{M}$ values as we increase the q value and this variation is reflected in the gradual increase of $\Delta\Phi$. Incidentally, this pattern is also observed for configurations having somewhat smaller initial dominant SO misalignments. However, the $\mathcal{M}$ estimates are close to unity for tiny $\tilde{\theta}_1(x_0)$ values and this is expected as precessional effects are minimal for such binaries. Therefore, the effect of the above discussed additional 3PN order terms are more pronounced for high mass ratio compact binaries having *moderate* dominant SO misalignments.

We find that the match estimates are less than the optimal 0.97 value for a non-negligible fraction of unequal mass spinning compact binaries. It may be recalled that such an optimal match value roughly corresponds to a 10% loss in the ideal event rate. We, therefore, conclude that the additional 3PN order terms in frequency and phase evolution equations in our approach should not be neglected for a substantial fraction of unequal mass binaries.

References

[1] Sathyaprakash B S and Schutz B F 2009 *Living Rev. Relativity* **12**
[2] Blanchet L 2006 *Living Rev. Relativity* **9** 4
[3] Blanchet L, Damour T, Esposito-Farese G and Iyer B R 2004 *Phys. Rev. Lett.* **93** 091101
[4] Blanchet L, Faye G, Iyer B R and Sinha S, 2008 *Class. Quantum Grav.* **25** 165003
[5] Barker B and O'Connell R 1975 *Phys. Rev. D* **12** 329
[6] Kidder L 1995 *Phys. Rev. D* **52** 821
[7] Apostolatos T A, Cutler C, Sussman G J and Thorne K 1994 *Phys. Rev. D* **49** 6274
[8] Buonanno A, Faye G and Hinderer T 2013 *Phys. Rev. D* **87** 044009; references therein
[9] http://www.ligo.org/index.php
[10] Buonanno A, Chen Y and Vallisneri M 2003 *Phys. Rev. D* **67** 104025
[11] Gupta A and Gopakumar A 2014 *Class. Quantum Grav.* **31** 065014, arXiv:1308.1315
[12] Gupta A and Gopakumar A 2015 *Class. Quantum Grav.* **32** 175002, arXiv:1507.00406.
[13] Bohe A, Marsat S and Blanchet L 2013 *Class. Quantum Grav.* **30** 135009
[14] Damour T, Iyer B R and Sathyaprakash B S 1998 *Phys. Rev. D* **57** 885